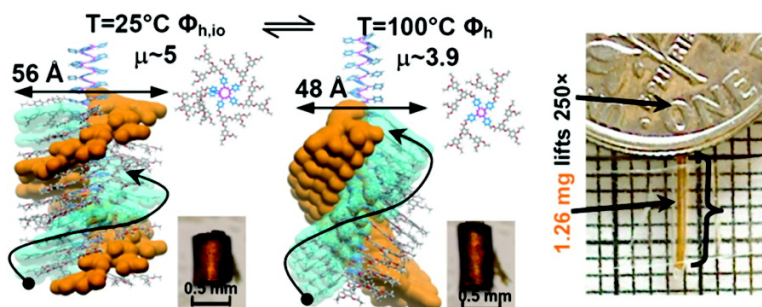Article

Nanomechanical Function from Self-Organizable Dendronized Helical Polyphenylacetylenes

Virgil Percec, Jonathan G. Rudick, Mihai Peterca, and Paul A. Heiney

More About This Article

Additional resources and features associated with this article are available within the HTML version:

- Supporting Information
- Links to the 8 articles that cite this article, as of the time of this article download
- Access to high resolution figures
- Links to articles and content related to this article
- Copyright permission to reproduce figures and/or text from this article

View the Full Text HTML

Nanomechanical Function from Self-Organizable Dendronized Helical Polyphenylacetylenes

Virgil Percec,*,[†] Jonathan G. Rudick,[†] Mihai Peterca,[†,‡] and Paul A. Heiney[‡]

Roy & Diana Vagelos Laboratories, Department of Chemistry, University of Pennsylvania, Philadelphia, Pennsylvania 19104-6323 and Department of Physics and Astronomy, University of Pennsylvania, Philadelphia, Pennsylvania, 19104-6396

Received March 12, 2008; E-mail: percec@sas.upenn.edu

Abstract: Self-organizable dendronized helical polymers provide a suitable architecture for constructing molecular nanomachines capable of expressing their motions at macroscopic length scales. Nanomechanical function is demonstrated by a library of self-organized helical dendronized cis-transoidal polyphenylacetylenes (*cis*-PPAs) that possess a first-order phase transition from a hexagonal columnar lattice with internal order (ϕ_h^{io}) to a hexagonal columnar liquid crystal phase (ϕ_h). These polymers can function as nanomechanical actuators. When extruded as fibers, the self-organizable dendronized helical *cis*-PPAs form oriented bundles. Such fibers have been shown capable of work by displacing objects up to 250-times their mass. The helical *cis*-PPA backbone undergoes reversible extension and contraction on a single molecule length scale resulting from cisoid-to-transoid conformational isomerization of the *cis*-PPA. Furthermore, we clarify supramolecular structural properties necessary for the observed nanomechanical function.

Introduction

Molecular architectures capable of undergoing stimulated, large amplitude directional motion between two or more components (i.e., nanomechanical function) have begun to fill a toolbox of molecular machines available to the nanosciences.[1] Interest in nanomechanical functions is inspired by Nature, wherein complex molecular machinery performs mechanical operations.[2] Such biological nanomachines can be coerced into artificial systems,[3] thus providing access to complexity currently unavailable in synthetic nanomachines. Wholly artificial molecular nanomachines have been shown to operate in solution,[4] at interfaces,[5,6] and in solid state.[7] Examples of such nanomachines include pistons,[4a] ratchets,[4b,c] rotors,[4d] elevators,[4e] motors,[4f,5c] pedals,[4g] springs,[4h] and nanocars.[5d] Reducing such imaginative designs to practice and controlling their directional motion represent two of the most fundamental challenges for developing molecular nanomachines.[1] A third challenge emerges as we recognize that Nature is able to translate work done by biomolecular machines into macroscopic output.

† Department of Chemistry.
‡ Department of Physics and Astronomy.

(1) (a) Kay, E. R.; Leigh, D. A.; Zerbetto, F. *Angew. Chem., Int. Ed.* **2007**, *46*, 72–191. (b) Browne, W. R.; Feringa, B. L. *Nat. Nanotech.* **2006**, *1*, 25–35. (c) Saha, S.; Stoddart, J. F. *Chem. Soc. Rev.* **2007**, *36*, 77–92. (d) Champin, B.; Mobian, P.; Sauvage, J.-P. *Chem. Soc. Rev.* **2007**, *36*, 358–366. (e) Shirai, Y.; Morin, J.-F.; Sasaki, T.; Guerrero, J. M.; Tour, J. M. *Chem. Soc. Rev.* **2006**, *35*, 1043–1055. (f) Garcia-Garibay, M. A. *Proc. Natl. Acad. Sci. U.S.A.* **2005**, *102*, 10771–10776. (g) Balzani, V.; Credi, A.; Venturi, M. *Molecular Devices and Machines - A Journey into the Nano World*; Wiley-VCH: Weinheim, 2003. (h) Kottas, G. S.; Clarke, L. I.; Horinek, D.; Michl, J. *Chem. Rev.* **2005**, *105*, 1281–1376.

(2) (a) Schliwa, M.; Woehlke, G. *Nature* **2003**, *422*, 759–765. (b) Oster, G.; Wang, H. *Trends Cell. Biol* **2003**, *13*, 114–121. (c) Doyle, D. A.; Cabral, J. M.; Pfuetzner, R. A.; Kuo, A.; BGulbis, J. M.; Cohen, S. L.; Chait, B. T.; MacKinnon, R. *Science* **1998**, *280*, 69–77. (d) Oldham, M. L.; Khare, D.; Quiocho, F. A.; Davidson, A. L.; Chen, J. *Nature* **2007**, *450*, 515–522.

(3) (a) Astier, Y.; Bayley, H.; Howorka, S. *Curr. Opin. Chem. Biol.* **2005**, *9*, 576–584. (b) Soong, R. K.; Bachand, G. D.; Neves, H. P.; Olkhovets, A. G.; Craighead, H. G.; Montemagno, C. D. *Science* **2000**, *290*, 1555–1558. (c) Liu, H.; Schmidt, J. J.; Bachand, G. D.; Rizk, S. S.; Looger, L. L.; Hellinga, H. W.; Montemagno, C. D. *Nat. Mater.* **2002**, *1*, 173–178. (d) Wolfe, A. J.; Mohammad, M. M.; Cheley, S.; Bayley, H.; Movileau, L. *J. Am. Chem. Soc.* **2007**, *129*, 14034–14041. (e) Kumar, M.; Grzelakowski, M.; Zilles, J.; Clark, M.; Meier, W. *Proc. Natl. Acad. Sci. U.S.A.* **2007**, *104*, 20719–20724. (f) Koçer, A.; Walko, M.; Meijberg; Feringa, B. L. *J. Am. Chem. Soc.* **2005**, *309*, 755–758.

(4) (a) Ashton, P. R.; Balzani, V.; Kocian, O.; Prodi, L.; Spencer, N.; Stoddart, J. F. *J. Am. Chem. Soc.* **1998**, *120*, 11190–11191. (b) Kelly, T. R.; De Silva, G.; Silva, R. A. *Nature* **1999**, *401*, 150–152. (c) Koumura, N.; Zijlstra, R. W. J.; van Delden, R. A.; Harada, N.; Feringa, B. L. *Nature* **1999**, *401*, 152–155. (d) Leigh, D. A.; Wong, J. K. Y.; Dehez, F.; Zerbetto, F. *Nature* **2003**, *424*, 174–179. (e) Badjic, J. D.; Balzani, V.; Credi, A.; Silvi, S.; Stoddart, J. F. *Science* **2004**, *303*, 1845–1849. (f) Balzani, V.; Clemente-León, M.; Credi, A.; Ferrer, B.; Venturi, M.; Flood, A. H.; Stoddart, J. F. *Proc. Natl. Acad. Sci. U.S.A.* **2006**, *103*, 1178–1183. (g) Muraoka, T.; Kinbara, K.; Aida, T. *Nature* **2006**, *440*, 512–515. (h) Kim, H.-J.; Lee, E.; Park, H.-s.; Lee, M. *J. Am. Chem. Soc.* **2007**, *129*, 10994–10995.

(5) (a) Shigekawa, H.; Miyake, K.; Sumaoka, J.; Harada, A.; Komiyama, M. *J. Am. Chem. Soc.* **2000**, *122*, 5411–5412. (b) Hernandez, R.; Tseng, H.-R.; Wong, J. W.; Stoddart, J. F.; Zink, J. I. *J. Am. Chem. Soc.* **2004**, *126*, 3370–3371. (c) Zheng, X.; Miulcahy, M. E.; Horinek, D.; Galeotti, F.; Magnera, T. F.; Michl, J. *J. Am. Chem. Soc.* **2004**, *126*, 4540–4542. (d) Shirai, Y.; Osgood, A. J.; Zhao, Y.; Kelly, K. F.; Tour, J. M. *Nano Lett.* **2005**, *5*, 2330–2334. (e) Nguyen, T. D.; Liu, Y.; Saha, S.; Leung, K. C.-F.; Stoddart, J. F.; Zink, J. I. *J. Am. Chem. Soc.* **2007**, *129*, 626–634.

(6) Liu, Y.; Flood, A. H.; Bonvallet, P. A.; Vignon, S. A.; Northrop, B. H.; Tseng, H.-R.; Jeppesen, J. O.; Huang, T. J.; Brough, B.; Baller, M.; Magonov, S.; Solares, S. D.; Goddard, W. A.; Ho, C.-M.; Stoddart, J. F. *J. Am. Chem. Soc.* **2005**, *127*, 9745–9759.

(7) Dominguez, Z.; Khuong, T.-A. V.; Dang, H.; Sanrame, C. N.; Nuñoz, J. E.; Garcia-Garibay, M. A. *J. Am. Chem. Soc.* **2003**, *125*, 8827–8837.
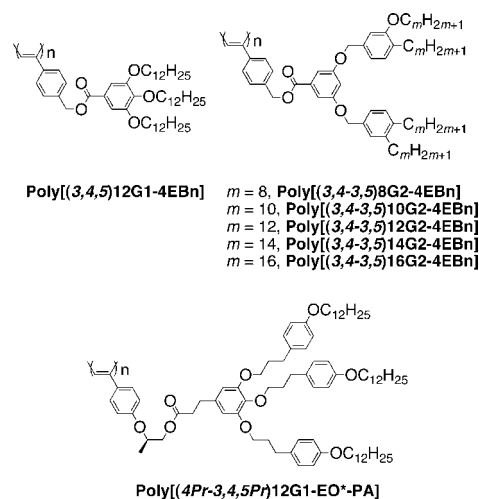
Two recent examples have illustrated strategies whereby the work done by molecular nanomachines manifests as changes at a dramatically larger length-scale. Stoddart, Ho, and co-workers have shown that unoriented molecular muscles in a self-assembled monolayer act in concert to deflect a Au-coated cantilever by tens of nanometers.[6] The molecular muscles are bistable [3]rotaxanes whose two macrocycles are mounted to the Au surface. Feringa, Broer, and co-workers have shown that rotation of a molecular nanomotor can be amplified in a cholesteric liquid crystal matrix to effect rotary motion of a 27 μm long glass rod sitting atop the liquid crystal film.[8] Rotation of the molecular motor alters the helical pitch of the cholesteric liquid crystal phase. These examples demonstrate that the potential to harness molecular mechanical power depends, at least in part, on the distance over which directional motions can be obtained cooperatively.

Self-organizable dendronized polymers[9–11] are expected to provide a suitable architecture for constructing molecular nanomachines capable of expressing their motions at even larger length-scales. These polymers were suggested to adopt a helical conformation.[11] They form oriented bundles, and their persistence length can be adjusted by the proper selection of dendritic side chain.[11] Alternatively, short polymer chains have been shown to self-assemble end-to-end forming very long single-macromolecule-wide strands.[12] Herein we demonstrate that the thermoreversible cisoidal-to-transoidal conformational isomerism[13] of dendronized helical *cis*-polyphenylacetylenes (*cis*-PPAs) creates a nanomechanical actuator in bulk and manifests as macroscopic work. Furthermore, we clarify supramolecular structural properties necessary for the observed nanomechanical function.

Results and Discussion

Controlled, Directional Motion Fueled by Thermal Energy. We have recently reported the synthesis, structural, and retrostructural analysis of 27 dendronized helical poly-arylacetylenes.[13,14] These polymers have demonstrated that the helical conformation of polymers jacketed with self-assembling dendrons[11] can be selected by chiral information from the dendritic side chains.[10] From this library, we have found seven examples of dendronized *cis*-PPAs that undergo thermorevers-

(8) Vicario, J.; Katsonis, N.; Ramon, B. S.; Bastiaansen, C. W. M.; Broer, D. J.; Feringa, B. L. *Nature* **2006**, *440*, 163.
(9) Percec, V. *Phil. Trans. R. Soc. A* **2006**, *364*, 2709–2719.
(10) Rudick, J. G.; Percec, V. *New J. Chem.* **2007**, *31*, 1083–1096.
(11) (a) Kwon, Y. K.; Chvalun, S.; Schneider, A.-I.; Blackwell, J.; Percec, V.; Heck, J. A. *Macromolecules* **1994**, *27*, 6129–6132. (b) Kwon, Y. K.; Chvalun, S.; Blackwell, J.; Percec, V.; Heck, J. A. *Macromolecules* **1995**, *28*, 1552–1558. (c) Percec, V.; Anh, C.-H.; Ungar, G.; Yeardley, D. J. P.; Möller, M.; Sheiko, S. S. *Nature* **1998**, *391*, 161–164. (d) Percec, V.; Anh, C.-H.; Cho, W.-D.; Jamieson, A. M.; Kim, J.; Leman, T.; Schmidt, M.; Gerle, M.; Möller, M.; Prokhorova, S. A.; Sheiko, S. S.; Cheng, S. Z. D.; Zhang, A.; Ungar, G.; Yeardley, D. J. P. *J. Am. Chem. Soc.* **1998**, *120*, 8619–8631.
(12) (a) Percec, V.; Rudick, J. G.; Wagner, M.; Obata, M.; Mitchell, C. M.; Cho, W. D.; Magonov, S. N. *Macromolecules* **2006**, *39*, 7342–7351. (b) Percec, V.; Holerca, M. N.; Magonov, S. N.; Yeardley, D. J. P.; Ungar, G.; Duan, H.; Hudson, S. D. *Biomacromolecules* **2001**, *2*, 706–728.
(13) (a) Percec, V.; Rudick, J. G.; Peterca, M.; Wagner, M.; Obata, M.; Mitchell, C. M.; Cho, W.-D.; Balagurusamy, V. S. K.; Heiney, P. A. *J. Am. Chem. Soc.* **2005**, *127*, 15257–15264. (b) Percec, V.; Rudick, J. G.; Peterca, M.; Staley, S. R.; Wagner, M.; Obata, M.; Mitchell, C. M.; Cho, W.-D.; Balagurusamy, V. S. K.; Lowe, J. N.; Glodde, M.; Weichold, O.; Chung, K. J.; Ghionni, N.; Magonov, S. N.; Heiney, P. A. *Chem. Eur. J.* **2006**, *12*, 5731–5746. (c) Percec, V.; Peterca, M.; Rudick, J. G.; Aqad, E.; Imam, M. R.; Heiney, P. A. *Chem. Eur. J.* **2007**, *13*, 9572–9581.

Scheme 1

Poly[(*3,4,5*)12G1-4EBn]

m = 8, **Poly[(*3,4-3,5*)8G2-4EBn]**
m = 10, **Poly[(*3,4-3,5*)10G2-4EBn]**
m = 12, **Poly[(*3,4-3,5*)12G2-4EBn]**
m = 14, **Poly[(*3,4-3,5*)14G2-4EBn]**
m = 16, **Poly[(*3,4-3,5*)16G2-4EBn]**

Poly[(*4Pr-3,4,5Pr*)12G1-EO*-PA]

ible cisoid-to-transoid conformational isomerism (Scheme 1).[13] Models for the cisoid and transoid conformations of a representative dendronized PPA (poly[(*3,4-3,5*)12G2-4EBn]) are presented in Figure 1a,b. This process corresponds to a stretching of the helical backbone upon heating and contraction upon cooling as observed by circular dichroism (CD) spectroscopy and X-ray diffraction (XRD) experiments.[13] We envision this reversible motion to be that of a molecular actuator. Thermal energy is the fuel, unwinding of the helix serves as the motor, and the supramolecular columnar dendritic coat serves as a casing to ensure the directionality of the *cis*-PPA backbone movement.

The first-order transition between an internally ordered hexagonal columnar phase (ϕ_h^{io}) and a hexagonal columnar (ϕ_h) liquid crystal phase is diagnostic for conformational isomerism. This phase transition is usually observed by differential scanning calorimetry (DSC).[13] XRD experiments confirm the larger column diameter (D_{col}) and helical features of the cis-cisoidal dendronized PPA in the ϕ_h^{io} phase. Figure 1c shows a plot of the experimental column diameter from XRD experiments of dendronized PPAs poly[(*3,4-3,5*)mG2-4EBn] of varied alkyl chain lengths on the periphery of the dendron (m = 8, 10, 12, 14, and 16). Figure 1 presents wide-angle XRD patterns for oriented fiber samples. Long-range helical features corresponding to correlations within the column are highlighted in the ϕ_h^{io} phase (Figure 1a). They are absent in the ϕ_h diffraction pattern (Figure 1b). Models consistent with these experimental results indicate that the reversible first-order transition corresponds to an extension along the column axis upon heating wherein the helical backbone unwinds.[13] Upon cooling from the ϕ_h phase, the column diameter increases and the helical features characteristic of the ϕ_h^{io} are observed. This demonstrates the reversibility of the unwinding−winding process of the helical structure.

Contraction of the column diameter and stretching along the column axis of a dendronized polymethacrylate exhibiting

(14) (a) Percec, V.; Obata, M.; Rudick, J. G.; De, B. B.; Glodde, M.; Bera, T. K.; Magonov, S. N.; Balagurusamy, V. S. K.; Heiney, P. A. *J. Polym. Sci., Part A: Polym. Chem.* **2002**, *40*, 3509–3533. (b) Percec, V.; Aqad, E.; Peterca, M.; Rudick, J. G.; Lemon, L.; Ronda, J. C.; De, B. B.; Heiney, P. A.; Meijer, E. W. *J. Am. Chem. Soc.* **2006**, *128*, 16365–16372. (c) Percec, V.; Rudick, J. G.; Peterca, M.; Aqad, E.; Imam, M. R.; Heiney, P. A. *J. Polym. Sci., Part A: Polym. Chem.* **2007**, *45*, 4974–4987.
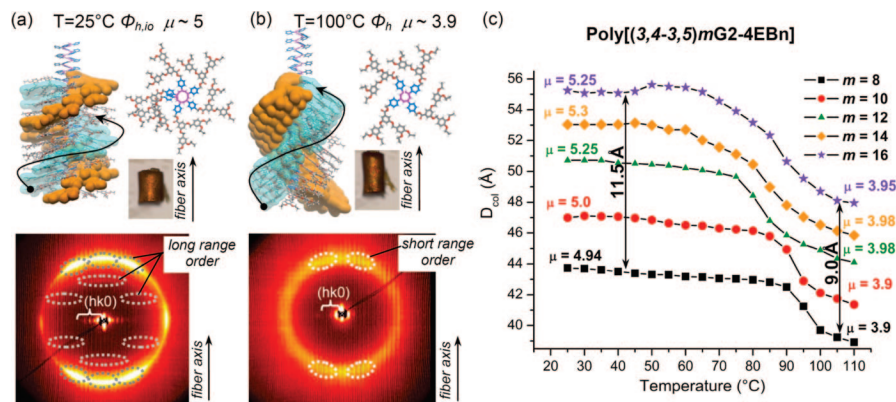
Figure 1. Schematic of the self-organizable dendronized helical *cis*-PPA in the (a) cisoid and (b) transoid conformations. (c) Temperature dependence of D_{col}. (a, b) poly[[(3,4-3,5)]16G2-4EBn] oriented fiber microscopy images and wide-angle XRD patterns depict the changes observed at macroscopic and microscopic scale between the two phases indicated.

a three-dimensionally ordered low temperature phase and ϕ_h phase at higher temperatures has be reported previously.[11b] While the process was found to be reversible, recovery of the three-dimensionally ordered phase was much slower than for the dendronized *cis*-PPAs. Furthermore, details of the backbone conformation remain uncertain for the previously reported dendronized polymethacrylate. A general model describing this process for two different types of polymer backbones has yet to be demonstrated.

Notably, the (un)winding process is temperature controlled. Each of the D_{col} values reported in Figure 1c are samples equilibrated at the specified temperature. Thermal energy, therefore, serves as the fuel for this nanomechanical actuator and determines the extent of displacement achieved. A distinguishing feature of these dendronized *cis*-PPAs from other dynamic helical polymers is that the supramolecular columnar dendritic coat prohibits the polymer backbone from collapsing into a globular conformation. Therefore, the backbone is restricted to conformational changes that only occur along the column axis.

Translating Molecular Movement to Macroscopic Loads. Orienting the nanomechanical actuators provides a means by which to harness their individual motions and accomplish work at significantly larger length scales. Stoddart, Ho, and co-workers acknowledge that their artificial molecular muscles operate with suboptimal efficiency since the molecular axes are not all collinear.[6] Despite having room to improve the efficiency of their artificial molecular muscles, the groups have demonstrated significant ability to utilized billions of molecular actuators to deflect a cantilever several tens of nanometers from its resting position.[6] Self-organizable dendronized polymers are preprogrammed to generate oriented domains of hexagonally packed cylindrical macromolecules in bulk and on surfaces.[11] We have previously shown by atomic force microscopy (AFM) that unoriented monolayers of short self-organizable dendronized polymers self-assemble into long molecular fibers and self-organize into large columnar monodomains.[12] Fibers extruded in the liquid crystalline melt generate macroscopic samples of the dendronized polymers (optical micrographs are shown as insets in Figure 1a,b), wherein the fiber axis and cylinder axis are the same. Furthermore, the inset micrographs show that the fiber expands along its axis when heated above the first-order phase transition temperature.

Extruded fibers of the dendronized PPAs orient the cylindrical polymers along the fiber axis. Fibers such as these are typically

used for structural and retrostructural analysis by XRD. Figure 1a,b shows wide-angle XRD patterns of oriented fiber samples. The fiber axis is noted in the figure. Reflections corresponding to the helix pitch and dendron tilt angle are highlighted. These features are internal correlations within a single column, whereas reflections perpendicular to the fiber axis relate to intercolumnar features. Similar diffraction patterns have been obtained for each of the dendronized polymers designated in Scheme 1, as well as for oriented fiber samples of a dendronized polymethacrylate.[11b] Thus, extrusion is a simple means by which we can generate nanomechanical components from self-organizable dendronized helical *cis*-PPAs for integration into larger devices.

It is important to note that D_{col} reported in Figure 1c and elsewhere is calculated based on the small-angle powder XRD experiments that provide $D_{col} = a$, where a is the ϕ_h lattice dimension calculated using $a = 2(d_{10} + \sqrt{3}d_{11} + 2d_{20})/3$, and d_{hk} are the (hk) reflection d-spacings. To study the effect of orientation on the column diameter for the poly[(3,4-3,5)mG2-4EBn] series both powder and fiber small-angle XRD temperature scans were performed. Within the experimental error there was no difference between the column diameters calculated from powder or oriented fiber XRD experiments. This comparison confirms that the observed thermal decrease of the lattice dimension with the increase of temperature (or the reverse trend upon cooling) is not an effect dependent on the macroscopic orientation of the sample. In other words, this study demonstrates that the oriented fibers preserve the structure of the dendronized *cis*-PPA from the powder state.

Extruded fibers of self-organizable dendronized helical *cis*-PPAs exhibiting a $\phi_h{}^{io}$-to-ϕ_h phase transition undergo anisotropic thermal expansion along the length of the fiber, while the diameter contracts. Figure 2 illustrates a complete heating cycle for a fiber of poly[(4Pr-3,4,5Pr)12G1-EO*-PA]. Similar figures for each of the other six dendronized *cis*-PPAs are included in the Supporting Information. Figure 3 illustrates four examples of macroscopic extension of nanomechanical dendronized *cis*-PPAs with the corresponding analysis for the change in length corresponding to temperatures above and below the $\phi_h{}^{io}$-to-ϕ_h phase transition. Similar anisotropic fiber expansion has been demonstrated for a dendronized polymethacrylate exhibiting a three-dimensionally ordered low temperature phase and ϕ_h phase at higher temperatures.[11b] Measurement of the fibers in the optical micrographs reveals a 29–45% increase in length (L_{OM})
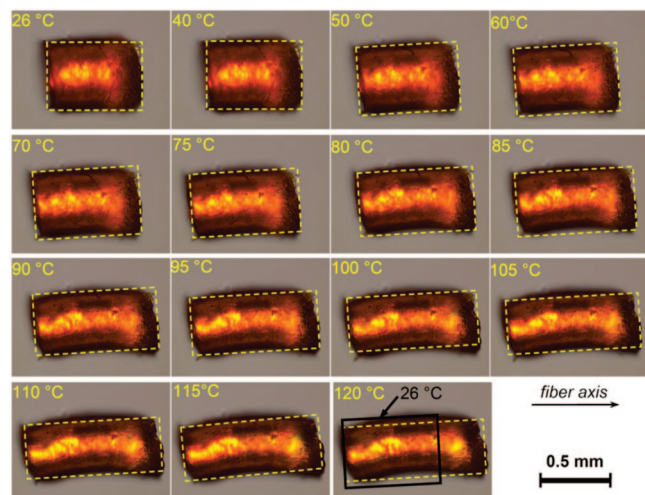
Figure 2. Transmission optical microscographs of the poly[(*4Pr*-3,4,5*Pr*)12G1-EO*-PA] oriented fiber collected upon heating at the indicated temperatures. The dotted-line box in each image denotes the region of the fiber used to measure the change in length.
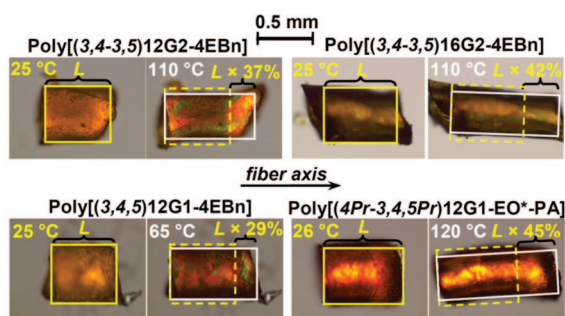

Figure 3. Transmission optical microscopy images collected on oriented fibers upon heating at the indicated temperatures. Percentage increases of fiber length (*L*) are marked. On cooling the exact reverse process (i.e., contraction) was observed.

as the sample temperature increases. Cooling the fiber samples resulted in a contraction to their original length. The nanomechanical actuators act in concert when extruded as fibers. This translates into macroscopic mechanical action.

In order to demonstrate that the individual cylindrical dendronized polymer actuators can perform in concert, we have shown that extruded fibers can lift macroscopic objects. Figure 4 shows an extruded fiber of poly[(*3,4-3,5*)16G2-4EBn] lifting a dime up an 8° incline. The fiber lifts 250-times its weight (Figure 4). Per repeat unit this constitutes a miniscule amount of work. We have developed a strategy whereby self-organizable dendronized *cis*-PPAs are able to create molecular actuators whose work is amplified to move macroscopic objects. This approach addresses the challenge of orienting nanomechanical actuators[6] and adds to the repertoire of nanomachines amenable to integration with larger-scale components.[6,8]

Tuning Molecular Motion through Dendron Structure. To further demonstrate that the nanomechanical behavior observed for individual dendronized polymers and macroscopic work we observe are in fact related, we have compared the change in length of an individual macromolecule in bulk determined from XRD experiments (L_{XRD}) to the change in length determined by optical microscopy (L_{OM}). We refer to L_{XRD} as the microscopic change in length and to L_{OM} as the macroscopic change in length. We can rearrange the geometric formula for the
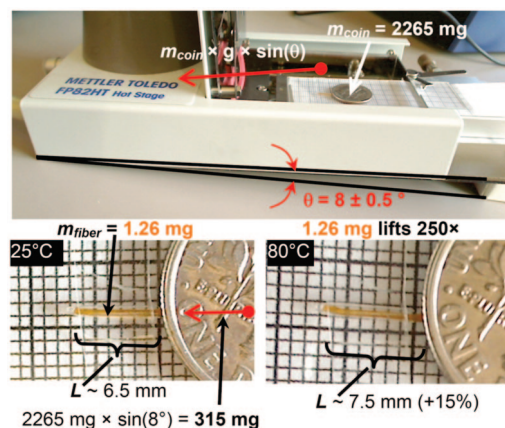

Figure 4. Experimental setup that demonstrates the macroscopic scale expansion and contraction of the oriented fiber by the lifting of a dime on the inclined plane of a Mettler hot stage (top). Expanded images collected by a digital camera at 25 °C (bottom left side) and at 80 °C (bottom right side) of the oriented fiber generated from poly[(*3,4-3,5*)16G2-4EBn] during lifting of 250-times its weight, via thermally fueled unwinding of its helix at the ϕ_h^{io}-to-ϕ_h transition.

volume of a cylinder (V_{col}) such that $L_{XRD} = 4V_{col}/(\pi D_{col}^2)$. Assuming the density ($\rho$) remains constant (i.e., $V_{col} = \rho/MW$ is constant for a given sample) over the temperature range investigated, we can see that $L_{XRD} \propto 1/D_{col}^2$. Using this relationship we compare the percentage change in L_{XRD} to that of L_{OM} (Figure 5). It is evident that the two phenomena are concurrent and that the extension profile depends on the structure of the dendronized helical *cis*-PPA.

The observed differences between L_{XRD} and L_{OM} at high temperatures in Figure 5 cannot be assigned definitively. The assumption that ρ is constant throughout the experiment is one possible explanation. The observed difference would imply that the density of the material increases slightly at higher temperatures, which is uncommon. Since the ϕ_h^{io} lattice is composed of porous columns and ϕ_h phase is not,[13] we might envision an increase in density at higher temperature during ϕ_h^{io}-to-ϕ_h phase transition. Experimentally determined density values for self-organizable dendronized *cis*-PPAs do not discriminate between those possessing a ϕ_h^{io}-to-ϕ_h phase transition and those that do not.[13,14] More likely there is also a discrepancy between the temperature of the heating element and the sample in both the XRD and optical microscopy experiments. The precision of the dendronized PPA temperature is important and any slight increase gradient in the temperature between the sample and the heating element can easily explain the difference without the need of assuming a change in the fiber density. It is also important to remark that such a gradient difference would increase as the temperature increases. The accuracy of the two experiments does not permit at this time any definitive assessment regarding the variation of the fiber density as a function of temperature.

It was observed that there is a direct relationship between the thermal changes of D_{col} in the hexagonal[13,14] or rectangular[13c,14c] phases observed at microscopic scale in the XRD experiments and the macroscopic scale thermal expansion/contraction of the dendronized PPA oriented fibers at the macroscopic scale. The three families of dendronized *cis*-PPAs reported here (Scheme 1) were the only ones that exhibited a variation of the column diameter as a function of temperature due to the presence of both ϕ_h^{io} and ϕ_h phases. All the other previously reported self-organizable dendronized PPAs[13,14] did not exhibit any change
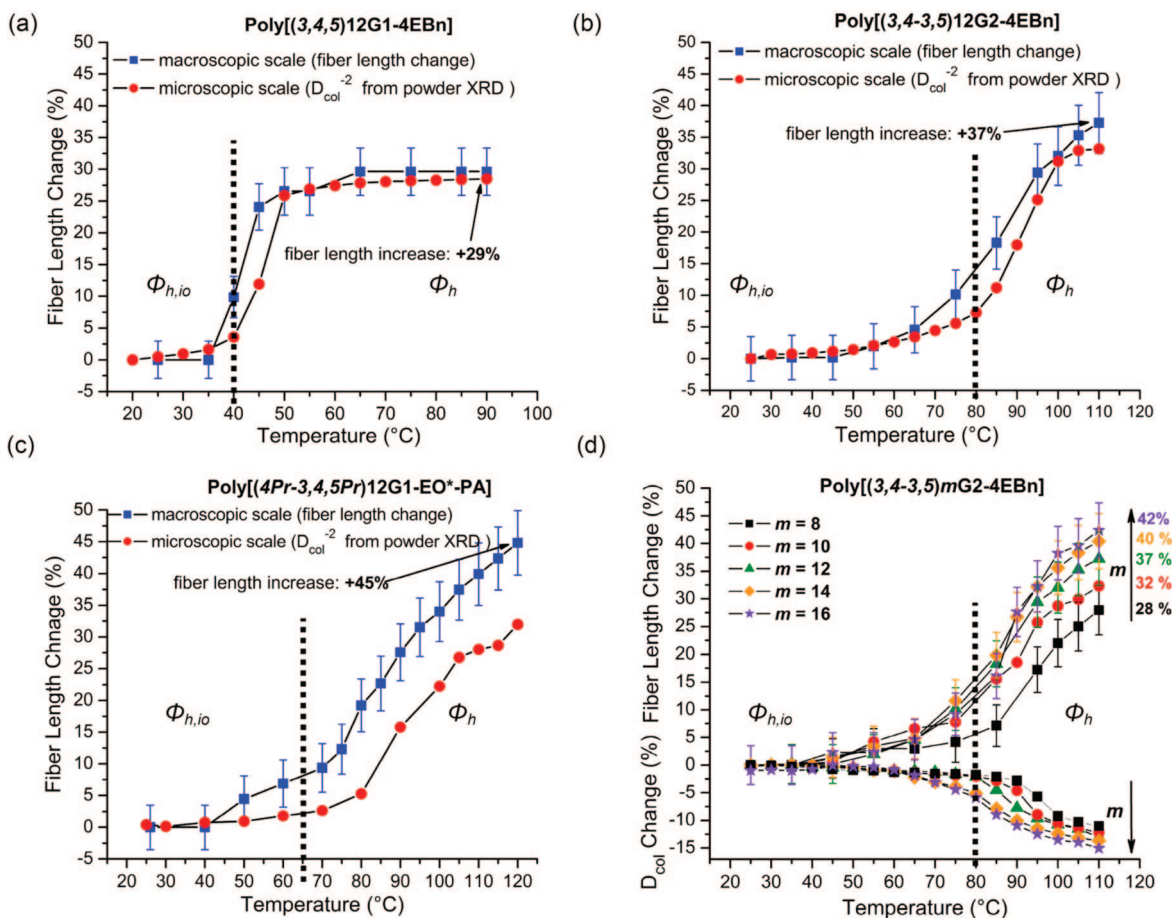
Figure 5. Scaled plots of the change in fiber length from optical microscopy (blue squares) and powder XRD experiments (red circles) as a function of temperature for the indicated dendronized *cis*-PPAs (a−c). The vertical dotted line indicates the $\phi_h{}^{io}$-to-ϕ_h transition temperature. Comparison of the fiber length change from optical microscopy and column diameter from powder XRD for the library of poly[(3,4-3,5)*m*G2-4EBn] from Scheme 1 (d). The arrows in d denote the direction of increasing peripheral alkyl chain length (*m*) for each of the two data sets.

of the oriented fiber as a function of temperature, in agreement with their XRD diffraction data.[13,14] This result demonstrates the important role of the dendron architecture toward the design of nanomechanical functions based on dendronized PPA.

Figure 5d shows the variation of the total extension as a function of peripheral alkyl tail length (*m*) for a single dendron substitution pattern. Larger *m* causes larger extensions of the helical polymer. The helical backbone stretches and the dendrons tilt more[13a] to better separate adjacent dendrons along the chain. The latter is evidenced by the decrease of the number of dendrons per column stratum (*μ*) in the ϕ_h phase compared to the $\phi_h{}^{io}$ phase (Figure 1c).[13a] Figure 1c reports *μ* calculated for the dendronized *cis*-PPAs poly[(3,4-3,5)*m*G2-4EBn].[13a]

The dendron architecture mediates formation of the $\phi_h{}^{io}$ phase, wherein the PPA backbone adopts a helical *cis*-cisoidal conformation,[13a,15] whereas the dendrons play a less determinant role in the polymer backbone conformation in the ϕ_h phase. *Cis*-cisoidal PPA is crystalline and corresponds to the more stable *cis*-PPA conformation.[15] Comparison of the different alkyl tail chain lengths (*m*) for poly[(3,4-3,5)*m*G2-4EBn] reveals that in the $\phi_h{}^{io}$ phase *μ* depends on the alkyl tail chain length. In the ϕ_h phase the values converge. Thus the dendron architecture templates the conformation of the polymer backbone in the $\phi_h{}^{io}$ phase. Furthermore, the difference between D_{col} for *m* = 8 and

m = 16 (from 11.5 Å at 20 °C to 9.0 Å at 100 °C) in the two phases further suggests that backbone conformation is more similar among the polymers in the ϕ_h phase regardless of *m*. These two observations imply that there is a cooperative mechanism between the dendron and the *cis*-PPA backbone. At low temperature the dendron architecture dominates the self-assembly process, whereas at high temperatures the *cis*-PPA backbone dominates this process and induces almost the same conformation, independent of the alkyl chain length.

The different expansion mediated by different *m* in the poly[(3,4-3,5)*m*G2-4EBn] series (Scheme 1) revealed the complex mechanism of the nanomechanical function. In the $\phi_h{}^{io}$ phase the reduced dendron freedom dictates a more compact packing and facilitate crystalline packing of the helical backbone. In the ϕ_h phase the dendrons frustrate the crystallization of the helical backbone. Nonetheless, the increased degrees of freedom of the dendritic part of the columns accommodate the backbone relaxation into a new minimum free energy configuration (i.e., an extended cis-transoidal helix). Consequently, the alkyl tail length study suggests allosteric regulation between the dendron and the backbone conformations.

Conclusion

In conclusion, self-organized helical dendronized PPAs that possess a $\phi_h{}^{io}$-to-ϕ_h phase transition can function as nanomechanical actuators. The helical PPA backbone undergoes revers-

(15) Simionescu, C. I.; Percec, V.; Dumitrescu, S. *J. Polym. Sci., Polym. Chem. Ed.* **1977**, *15*, 2497–2509.

ible extension and contraction on a single molecule length scale resulting from cisoid-to-transoid conformational isomerization of the *cis*-PPA. Oriented fiber samples manifest the behavior of the cylindrical macromolecules as anisotropic thermal expansion. Such fibers have been shown capable of work by displacing an object up to 250-times their mass. Oriented fibers of dendronized PPAs lacking a ϕ_h^{io}-to-ϕ_h phase transition do not exhibit macroscopic extension and contraction. Extension of this concept to other classes of dendronized polymers is under investigation.

Supporting Information Available: Supporting figures including experimental part and additional transmission optical micrographs of anisotropic fiber expansion. The material is available free of charge via the Internet at http://pubs.acs.org.

JA801863E